Conformal Transmitarray for Scan Loss Mitigation with Thinned Reconfiguration

T. A. Hill[1], J. R. Kelly[2], M. Khalily[1], T. W. C. Brown[1]
[1]Institute for Communication Systems, Home of the 5G Innovation Centre, University of Surrey
Guildford, UK, GU2 7XH, t.hill@surrey.ac.uk
[2]School of Electronic Engineering and Computer Science, Queen Mary University of London
London, UK, E1 4NS, j.kelly@qmul.ac.uk

***Abstract*—A conformal transmitarray with thinned control is presented, operating at 28 GHz. Its side panels are rotated to align with the maximum steering angle, increasing the gain and reducing the scan loss. The transmitarray is fed by an 8-element linear phased array antenna. Beam focusing to +/- 53 degrees is demonstrated for two different directions, using combinations of crossed-slot unit cells. A unit cell placement rule is proposed to significantly reduce (i.e. thin) the required number of reconfigurable unit cells. A filling factor of 43% was achieved compared to a fully populated design. This reduces the cost and biasing complexity. By minimising scan loss, this antenna could improve the performance of 5G small-cell access points.**

***Index Terms*—Phase shifting surface, active radome, millimeter wave antennas.**

I. Introduction

At millimetre wave frequencies, high gain and efficiency are essential to satify the link budget. However, scan loss limits the gain at wide steering angles, and the sidelobe level (SLL) must be minimised to reduce interference [1]. Future 5G networks will be based on densely-spaced small cells, so the cost of deployment is also a key concern.

A transmitarray is a periodic structure used to collimate a wavefront from a feeding antenna and thus produce a high gain beam [2]. Phase shifts are applied to the unit cells, between elements on the receive and transmit layers [3]. Unlike phased arrays, transmitarrays do not require a power-splitting network, so losses can be greatly reduced [4].

Typically, at each location on the surface of a fixed transmitarray, the unit cells are physically scaled in order to obtain the required amplitude and phase distribution. Thus, only one focusing direction is available. A reconfigurable transmitarray can retransmit incoming wavefront towards a desired beam direction. This is determined by electronically controlling the phase shift through each unit cell, sometimes implemented as a phase shifting layer [5]. PIN diodes can be used to enable fast phase reconfiguration with an insertion loss below 1 dB [4]. However, a large number of components is typically required, increasing the cost.

Due to having a finite projected area, the gain of a planar structure falls when steering to wide angles. The authors have been working on a non-planar lens arrangement was proposed to mitigate scan loss, but the lenses are bulky. This motivates the use of conformal transmitarrays [6]. In [7], a 400-element 3-facet transmitarray achieved a boresight directivity of 29.1 dBi, and a scan loss of around 2 dB for a panel tilt angle of 70°.

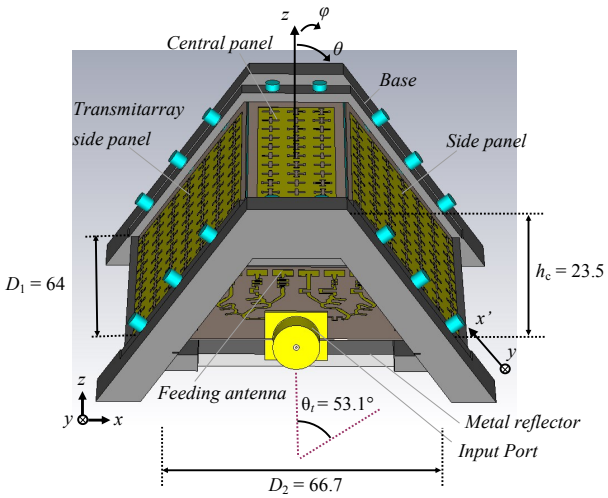

Fig. 1. Transmitarray structure.

A phased array can be used to feed a transmitarray, achieving a increased beam steering flexibility and a smaller form factor [8]. Thinning algorithms have been used to reduce the number of elements in phased arrays [9], but to the best of our knowledge these have not yet been applied to transmitarrays. Particle swarm optimisation enables the synthesis of transmitarrays with limited phase range, whilst still maintaining a low SLL [10]. However, this algorithm required 4000 iterations to converge to a solution, and cannot be expressed as a simple rule.

In this paper, we propose a beam steerable transmitarray with a reduced number of reconfigurable unit cells (thinned reconfiguration). Unlike a conventional transmitarray, the novel design, presented here, achieves reconfigurable focusing, but does not actively steer the radiated beam. This is instead performed by the phased array feeding antenna. The transmitarray focuses in the y direction whereas the phased array increases the gain in the x direction. Combining the two approaches yields a steerable spot beam. Each unit cell has reduced thickness and insertion loss compared with multilayer designs,

which are conventionally used to increase the phase shifting range. Within each panel, groups of unit cells are switched between two states to align the focusing direction with the main lobe of the feeding antenna. Regions away from the main lobe are filled with fixed unit cells. To implement this, we describe a unit cell placement rule, enabling the transmitarray to be designed to focus arbitrary feed radiation patterns.

The paper is structured as follows. Section II describes the unit cell design. Section III outlines the novel transmitarray design. Section IV presents simulation results, and concluding remarks are provided in Section V.

II. Unit Cell Design

Fig. 2 shows the structure of the 1-bit unit cell, which operates at 28 GHz. It is based on the design presented in [11]. It consists of two metal layers: the receive and transmit layer. These layers are printed on a Rogers® RT5880 substrate material having a thickness of 0.254 mm, a dielectric constant of 2.2, and a loss tangent of 0.0009. Each metal layer consists of a pair of crossed slots, and has thickness of 0.017 mm. As observed in [12], the symmetry of the unit cell shape enables them to be adapted for dual linear or circular polarisation. The incident fields are vertically polarised (E_y). The two metal layers are separated by a 3 mm thick layer of ePTFE material (of dielectric constant ϵ_r = 1.4), which creates a 100° phase shift between these layers.

The unit cell can be reconfigured between two phase states, OFF (0°) and ON (180°). For the ON state, it has a crossed-slot structure. In the OFF state, the slots are loaded with caps to create a Jerusalem-cross shape. This resonant element produces a large phase shift over a wide bandwidth [13], cancelling the phase shift through the layers. Electronic reconfiguration could be achieved by placing PIN diodes across the ends of the slots, and applying a different bias voltage for each state. DC blocking in the form of interdigital capacitors would be needed to isolate the voltages, and RF choke inductors would be needed at the ends of the bias lines. As a proof-of-concept, the transmitarray is demonstrated using fixed unit cells. The transmitarray could also be implemented using other unit cell shapes, for example, square loops.

The unit cell was simulated in CST Microwave Studio® using Floquet ports and the frequency domain solver. Fig. 3 shows the magnitude and phase of the E_y transmission through the unit cell in ON and OFF states. A phase change of 189° can be observed, which is close to 180°, and the transmission magnitude at 28 GHz is at least -1.76 dB for both states.

III. Transmitarray Design

The presented transmitarray features several modifications compared with a conventional design. These were necessary in order to maximise gain whilst minimising component cost.

Firstly, as it is a transmitarray with *thinned* control, reconfigurable unit cells are only placed in regions where a phase reversal is required. This contrasts with a transmitarray with *fully populated* control, in which all of the unit cells are

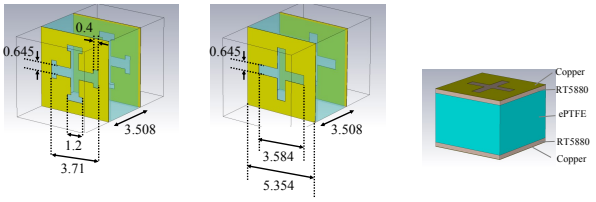

(a) (b) (c)

Fig. 2. Unit cell physical dimensions in mm. (a) OFF, (b) ON, (c) Layer stackup, showing 2 layers of copper.

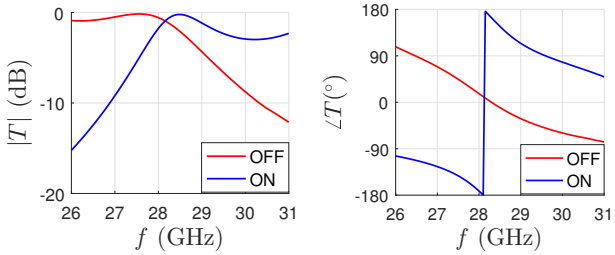

(a) (b)

Fig. 3. Unit cell transmission for ON and OFF states. (a) Magnitude, (b) Phase.

individually reconfigured using their own bias lines. Reducing the number of reconfigurable unit cells reduces the biasing complexity and component cost, at the expense of slightly reduced gain. This has some similarity with the method presented in [14].

Secondly, beam steering is performed primarily within the phased array feed, rather than at the transmitarray panels. This prevents truncation of the phase pattern and avoids the phase wrap problem described in [5], so it limits the SLL. When steering to the maximum angle, a progressive phase is applied to the central panel, but as the panel is thin, this does not cause a SLL increase. Although using a unit cell with a 1-bit phase resolution reduces the directivity by 3.92 dB [16] [3], the number of diodes is halved compared to a fully populated transmitarray. Using fewer substrate layers reduces the insertion loss and simplifies manufacture, at the expense of increased phase error and reduced directivity (and increased SLL) of the transmitarray. These design features enable the cost to be minimised whilst maintaining acceptable performance.

The transmitarray is fed by a previously designed phased array [15]. The feed array pattern can be approximated as G_{feed} (dBi) $= 10\log_{10}(\cos^{30}(\theta - 48°)\cos^4(\phi)) + 10.98$. For the side panels, f/D = 0.34 was selected to achieve maximum total efficiency, by balancing spillover efficiency (-0.26 dB = 94.2%) with taper efficiency (-1.01 dB = 79.2%). For feed exponent n = 4, the feed edge taper is -9.88 dB, and the subtended angle is 55.5°. The side panels were inclined by $\theta_t = 53°$ to align them with the maximum steering angles. For both panels, f = 22 mm. A metal plate reflector is located at a distance of $\frac{3\lambda_0}{4}$ = 8.03 mm behind the array elements.

The cutting height (h_c) of the central panel determines the

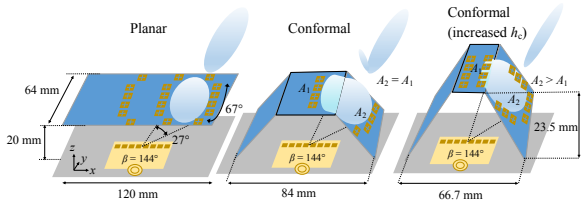

Fig. 4. Evolution of the transmitarray shape from planar to conformal. β is the progressive phase shift between the phased array elements.

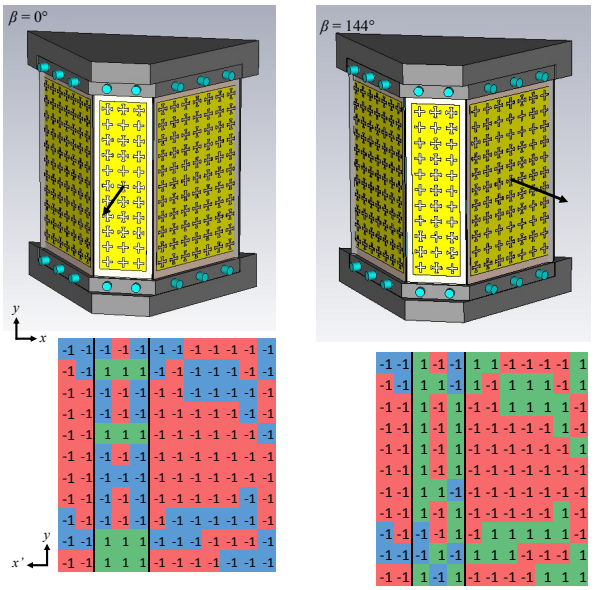

(a) (b)

Fig. 5. Transmitarray panels and unit cell combinations for each beam steering angle of the feed array. ON = green, OFF = blue, permanently OFF = red. (a) β = 0°, (b) β = 144°.

area (and hence gain) of each panel. The aim is to achieve a gain profile which is the reciprocal of the scan loss. Fig. 4 shows the evolution of the design from a flat panel to a conformal surface. Initially, panels with equal area were designed, but the gain at the maximum steering angle was not sufficient. Increasing the cutting height increased the area of the side panels, mitigating scan loss. This also helped to suppress sidelobes when beam steering to the maximum angle, as more of the radiation from the feed PCB was incident on the side panel. An attempt was initially made to thin the total number of unit cells, by producing a 180° phase shift relative to the blank dielectric layers, but this reduced the gain, as a smaller proportion of the panel area was populated with cells. Instead, thinning of the number of reconfigurable unit cells was proposed.

Now we describe a rule for determining the positions of the reconfigurable unit cells. As shown in Fig. 5, combinations of unit cells are switched ON or OFF to create the phase distributions required for each beam direction. Each unit cell has 3 possible states: ON, OFF, or permanently OFF. If a cell is not used for any beam steering directions, it is permanently OFF, and does not need to be reconfigured. Thinning with an amplitude constraint means that reconfigurable unit cells are placed in the illuminated region, where they are most needed.

When steering to the boresight (0°) direction (using the β = 0° feeding array), the feed array has already narrowed the beamwidth in azimuth, so unit cells only need to be placed to achieve elevation focusing. The central panel of the transmitarray is active, and the unit cells in the side panels are OFF (Fig. 5(a)).

When steering to +53° (using β = 144° in the feed), most of the feed radiation is incident on the side panel. The opposite side panel at -53° is OFF. However, as the side panels have been truncated, unit cells within the central panel are also used to form the correct phase distribution. A progressive phase (0°, 180°, 360°) is added across middle of the central panel to steer this part of the wavefront (Fig. 5(b)). The unit cells on the central panel are shared between all beam directions, so for this panel, a unit cell is reconfigurable if it changes state for any beam direction.

The panel design process is split into three steps. Firstly, within each transmitarray panel, the amplitude and phase of the incident field (E_y) must firstly be evaluated for the dielectric layers on their own (without copper). This is because the phase distribution of the waves incident on the transmitarray is a combination of effects from the radiating elements, power-splitting network, and transmitarray panel geometry. Secondly, the phase at the centre of the panel corresponding to the main lobe of the feed is used as the 0° reference. ON unit cells are placed along phase contours to ensure that the wavefronts emitted from the transmitarray are in phase. A reconfigurable unit cell is only placed where the amplitude of the incident field above a certain threshold. The unit cell placement rule is as follows:

$$\psi_{mn} = \begin{cases} 180° & \text{if } |E_y| \geq |E_y|_{min} \text{ and} \\ & \angle \mathrm{E}_{ymin} \leq \angle E_y \leq \angle E_{ymax} \\ 0° & \text{otherwise} \end{cases} \quad (1)$$

where ψ_{mn} is the required phase shift through unit cell (m,n). ψ_{mn} equates to $\Delta\angle E_{y,ON}$ = 180°, or $\Delta\angle E_{y,OFF}$ = 0°. $|E_y| = |E_y(x', y')|$ is the E-field amplitude in V/m and $\angle E_y = \angle E_y(x', y')$ is the phase in degrees.

For correct wrapping in the range -180° to +180°, the phase is calculated as $\angle E_y = (Re(E_y), Im(E_y))$.

Table I shows the threshold values used for each beam steering direction. A lower value of amplitude threshold $|E_y|_{min}$ is used for β = 144° because the magnitude of the fields incident at the edge of the panels is lower for this case.

TABLE I
AMPLITUDE AND PHASE THRESHOLDS FOR THE UNIT CELL PLACEMENT RULE.

β	$\lvert E_y\rvert_{min}$	$\angle E_{ymin}$	$\angle E_{ymax}$
0°	30 V/m	-230°	-50°
144°	5 V/m	-154°	+26°

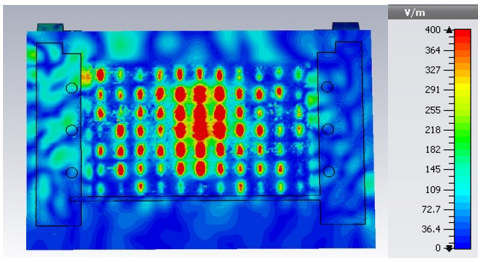

(a)

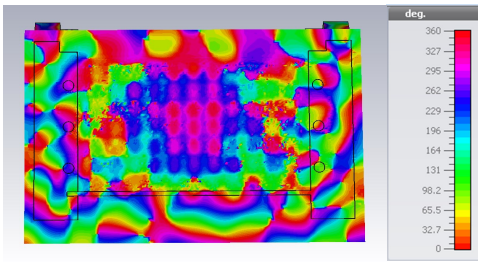

(b)

Fig. 6. Side panel with unit cells, fed by β = 144° array. (a) $|E_y|$, (b) $\angle E_y|$.

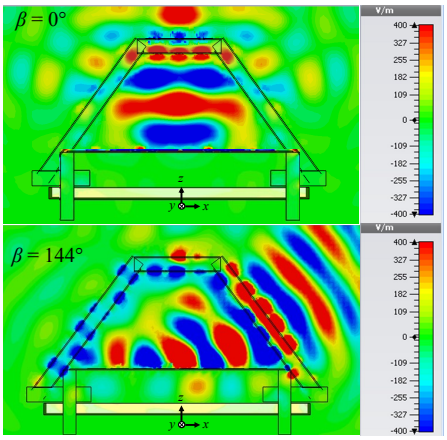

Fig. 7. $|E_y|$ cross sections through the transmitarray.

Thirdly, once the rule has been applied, E_y is evaluated in a coordinate system (x', y') local to each panel. For the central panel, $x' = -x$, whereas for the side panel, $x' = -0.8x+0.6z$, i.e. the coordinates are rotated by θ_t. For both panels, $y' = y$. The spacing between unit cells is $d = \lambda_0/2$ in both directions, x' and y', such that the unit cells form a regular grid ($x'_{mn} = md$, $y'_{mn} = nd$). Once the rule has been applied, the unit cell positions are mapped back onto the panels.

For the central panel, the required phase is $\angle E_y = \angle E_{y,feed} + \Delta\phi$, where $\angle E_{y,feed}$ is the phase of the feeding antenna on its own, and phase correction $\Delta\phi = k(-0.2x + 12)\sin\theta_t$. This correction is based on the $k\Delta d \sin\theta_t$ formula mentioned in [17]. The phase error was minimised by the correct placement of unit cells (Fig. 6(b)). The maximum phase error was 90° within the illuminated region.

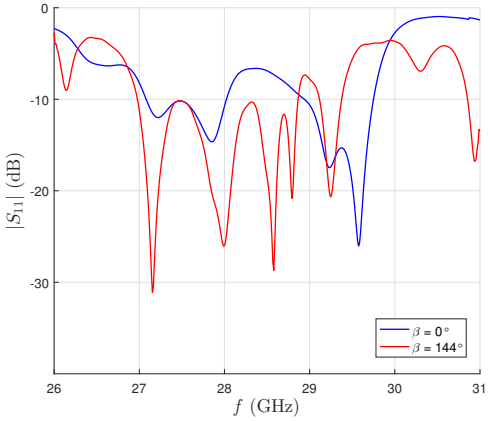

Fig. 8. Frequency variation of the reflection coefficient for β = 0°, β = 144°.

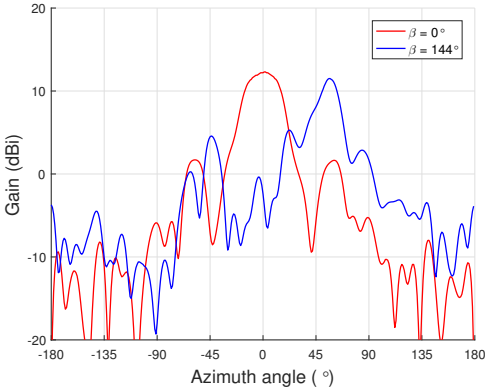

Fig. 9. Azimuth radiation patterns for β = 0°, β = 144°. The pattern cut is through the xoz plane.

The pattern of unit cells synthesised by the rule is known as the *population matrix*, as displayed earlier in Fig. 5. This matrix can be used within MATLAB® to predict the radiation pattern of each panel. Focusing primarily occurs along the y direction, as the phased array has already narrowed the beam in the x direction. Hence, a fan beam from the feeding antenna becomes a spot beam. The unit cell patterns (zones) are perpendicular to the direction of focusing.

The *filling factor* represents the proportion of the panel area which is covered by reconfigurable unit cells. It measures the reduction in the number of unit cells. The filling factor can be controlled by adjusting the amplitude and phase thresholds in the unit cell placement rule. For a given filling factor, the rule calculates the arrangement of unit cells which maximises the gain and limits the SLL. For the side panels, a filling factor of 35% was used, and for the central panel, the filling factor was 81%. The average filling factor was 43%, resulting in a total PIN diode cost reduction of 57% compared to a design with fully populated control.

IV. Results

The conformal transmitarray was simulated for two different beam directions in CST Microwave Studio® using the time

domain solver.

Fig. 7 shows the y-component of the E field on a cross-section through the structure. The wavefronts are focused as they pass through the transmitarray panels. When β = 0°, the elevation beamwidth reduced to 15.4° (compared to a beamwidth of 70° for the feeding antenna on its own), and for β = 144°, the elevation beamwidth reduced from 67° to 28°. A total efficiency of 75% was achieved for both beam steering directions. As seen in Fig. 8, a -10 dB return loss bandwidth of 0.9 GHz was achieved. This is sufficiently wide to enable 5G communications.

Fig. 9 shows the scanning performance of the transmitarray antenna. Compared to the conventional phased array on its own [15], the realised gain at +53° increased by 2.4 dB, and the scan loss has been reduced by 3.21 dB to just 0.2 dB. A sidelobe level less than -6 dB was achieved for steering angles 0° and ±53°. The side panels with OFF unit cells caused the SLL of the boresight radiation pattern to increase by 9 dB, and this could be further optimised in future work. The performance of the novel antenna is comparable with a fixed lens antenna, developed by the authors, which uses cascaded zone plate lenses. However, the novel design reported here has the advantage of a much smaller form factor.

V. Conclusion

The design of a beam steerable conformal transmitarray with thinned reconfiguration has been presented. Using a thinned arrangement, different combinations of unit cells are selected (turned ON or OFF), creating phase changes which are aligned with the beam direction of the feeding antenna. The number of reconfigurable unit cells (and hence PIN diodes and cost) was reduced by 57% to just 81 cells. A unit cell placement rule was devised to simplify the layout of the transmitarray panels. At the maximum steering angle of ±53°, the conformal structure ensured that the incident wavefronts are normal to the side panels, reducing scan loss to just 0.2 dB. A simulated gain of at least 11.9 dBi and a SLL below -6 dB were achieved for two different steering angles. Measurements of a fabricated prototype are in progress.

Acknowledgment

The authors would like to acknowledge the support of the EPSRC MILLIBAN project (EP/P008402/1) as well as the University of Surrey 5GIC (http://www.surrey.ac.uk/5gic).

References

[1] M. Rebato, L. Resteghini, C. Mazzucco and M. Zorzi, "Study of realistic antenna patterns in 5G mmwave cellular scenarios," in *Proc. 2018 IEEE International Conference on Communications (ICC)*, Kansas City, MO, 2018, pp. 1-6.

[2] B. Rahmati and H. R. Hassani, "High-efficient wideband slot transmitarray antenna," *IEEE Trans. Antennas Propag.*, vol. 63, no. 11, pp. 5149-5155, Nov. 2015.

[3] A. H. Abdelrahman, F. Yang, A. Z. Elsherbeni, and P. Nayeri, Analysis and Design of Transmitarray Antennas, Synthesis Lectures on Antennas, Vol. 6, No. 1, pp. 7-12, 39-47, Morgan Claypool, Jan. 2017.

[4] L. Di Palma, A. Clemente, L. Dussopt, R. Sauleau, P. Potier, and P. Pouliguen, "Circularly-polarized reconfigurable transmitarray in Ka-band with beam scanning and polarization switching capabilities," *IEEE Trans. Antennas Propag.*, vol. 65, no. 2, pp. 529–540, 2017.

[5] J. Y. Lau and S. V. Hum, "Reconfigurable transmitarray design approaches for beamforming applications," *IEEE Trans. Antennas Propag.*, vol. 60, no. 12, pp. 5679-5689, 2012.

[6] S. H. Zainud-Deen, S. M. Gaber, H. A. Malhet and K. H. Awadalla, "Cylindrical perforated transmitarrays," in *Proc. The 2nd Middle East Conference on Antennas and Propagation*, Cairo, Egypt, 2012, pp. 1-7.

[7] F. Diaby, A. Clemente, L. Dussopt, R. Sauleau, K. Pham, and E. Fourn, "Design of a 3-facet linearly-polarized transmitarray antenna at Ka-band," in *Proc. IEEE Int. Symp. Antennas Propag.*, Boston, MA, 2018. (in press)

[8] A. Abbaspour-Tamijani, L. Zhang, and H. Pan, "Enhancing the directivity of phased array antennas using lens-arrays," *Prog. Electromagn. Res.*, vol. 29, pp. 41-64, Feb. 2013.

[9] E. Tohidi, M. M. Nayebi and H. Behroozi, "Dynamic programming applied to large circular arrays thinning," *IEEE Trans. Antennas Propag.*, vol. 66, no. 8, pp. 4025-4033, Aug. 2018.

[10] J. Yu, L. Chen, J. Yang and X. Shi, "Design of a transmitarray using split diagonal cross elements With limited phase range," *IEEE Antennas and Wireless Propagation Letters*, vol. 15, pp. 1514-1517, 2016.

[11] A. H. Abdelrahman, F. Yang, A. Z. Elsherbeni, and A. Khidre, "Transmitarray antenna design using slot-type element," in *Proc. IEEE Int. Symp. Antennas Propag.*, Orlando, FL, 2013, pp. 1356-1357.

[12] S. A. Matos, E. B. Lima, J. R. Costa, C. A. Fernandes and N. J. G. Fonseca, "Generic formulation for transmit-array dual-band unit-cell design," in *Proc. 2017 11th European Conference on Antennas and Propagation (EuCAP)*, Paris, 2017, pp. 2791-2794.

[13] M. Jiang, Z. N. Chen, Y. Zhang, W. Hong and X. Xuan, "Metamaterial-based thin planar lens antenna for spatial beamforming and multibeam massive MIMO," *IEEE Trans. Antennas Propag.*, vol. 65, no. 2, pp. 464-472, Feb. 2017.

[14] S. L. Liu, X. Q. Lin, Z. Q. Yang, Y. J. Chen, and J. W. Yu, "A W band low profile transmitarray antenna using different types of FSS units," *IEEE Trans. Antennas Propag.*, vol. 66, no. 9, pp. 4613-4619, Sept. 2018.

[15] T. A. Hill, J. R. Kelly, "28 GHz Taylor feed network for sidelobe level reduction in 5G phased array antennas," *Microw. Opt. Technol. Lett.*, 2018. (in press)

[16] G. Ahmad, T. W. C. Brown, C. I. Underwood and T. H. Loh, "How coarse is too coarse in electrically large reflectarray smart antennas? A phase quantization case study at millimeter wave bands," in *Proc. IEEE International Workshop on Electromagnetics (iWEM)*, London, 2017, pp. 135-137.

[17] N. H. Noordin, T. Arslan and B. Flynn, "3-faceted array with low side lobe levels using tuneable windows," in *Proc. 2013 7th European Conference on Antennas and Propagation (EuCAP)*, Gothenburg, 2013, pp. 600-604.